HYPERSPECTRAL TECHNIQUES AND GIS FOR ARCHAEOLOGICAL INVESTIGATION

D. Emmolo, V. Franco, M. Lo Brutto, P. Orlando, B. Villa

Dipartimento di Rappresentazione, Università di Palermo Viale delle Scienze 90128 Palermo, Italy
bevilla@unipa.it, pietroorlando@dirap.unipa.it

Commission WG VII/4

KEY WORDS: Remote sensing, Archaeology, Cultural Heritage, Hyperspectral, Imagery, GIS.

ABSTRACT:

Aerial photos, both in colour and in black and white, have always been very important tools in archaeological surveys. Sensors, called hyperspectral, were available on the market for some years: they are able to expand the research beyond the visible area of the electromagnetic spectrum as far as the thermal infrared too.
The use of these sensors, at first restricted to the applications in the traditional fields of Remote Sensing (such as, for instance, Botany, Agronomy, Geology, Hydrology), was spreading, in recent years, to some sectors, such as archaeological surveys, which were unexplored before. The presence of structures and hollows in the top subsurface is likely to cause variations in humidity in the surface. These variations affect both vegetation, and some physical features of the ground such as thermal conductivity and capacity. Especially in the first hours of day, you can notice thermal anomalies due to different evaporation. The exam of these anomalies, carried out by the use of techniques of digital processing of images in the spectrum bands particularly sensitive to the above-mentioned indicators, enables the photointerpreter to determine possible signs of underground structures of archaeological interest.
The application of the remote sensing in archaeology allows to acquire, with rapidity, a lot of information connected to the territory; that’s the reason why, together with the development of sensors, came out the necessity to take advantage from the potentialities offered by the GIS to manage, process and file the spatial dates acquired with the remote sensing techniques. In this work, in fact, the results produced with the image processing technique were implemented in a GIS and were overlaid on the historical and contemporary maps and on the DEM in order to produce, for each study area, a *Prediction map of archaeological finds*.

1. INTRODUCTION

The spatial nature of archaeological data was recognized since more than a century and the same archaeology was defined as a spatial discipline. The diffusion of GIS inside the archaeological community happened in the last ten years in order to record, process and manage a lot of spatial data acquired using different methodologies of archaeological researches. Archaeology has adopted since time research methods and analysis instruments typical of scientific sectors as Geophysics, Topography, Photogrammetry and Remote Sensing. Recently especially Remote Sensing and GIS have taken a great importance. These technologies offer, through the overall study of the territory, an instrument for studying the relationship between community and belonging territory, processing and integrating the information of different origins collected during researches.
The Remote Sensing, thanks to the diffusion in the market of sensors called hyperspectral, allows to collect information on physical greatnesses on wide territory areas. The buried structures produce anomalies on some physical properties, as Thermal Inertia and Thermal Conductivity. The digital image processing allows to find these anomalies and permits the photointerpeter to individuate possible tracks of buried structures of archaeological interest. In this way it is possible to individuate areas on which direct other researches as geophysics.

2. STUDY AREA

An area in the province of Enna was chosen as test site. This part of Sicily is characterized by the presence of many archaeological sites; in particular the experimentation regarded the area around the “Villa del Casale” and the archaeological site of *Sofiana*. The Roman *Villa del Casale* was constructed on the remains of an older villa in the first quarter of the fourth century, probably as the centre of a huge latifundium covering the entire surrounding area. How long the villa kept this role is not known, maybe for less that 150 years, but the complex remained inhabited and a village grew around it, named *Platia*, derived from *Palatium*. It was damaged, maybe destroyed during the domination of the Vandals and the Visigoths, but the buildings remained in use, at least in part, during the Byzantine and Arab period. The site was abandoned for good when a landslide covered the villa in the 12th century CE, and remaining inhabitants moved to the current location of Piazza Armerina. The existence of the Villa was almost entirely forgotten (some of the tallest parts have always been above ground) and the area used for cultivation. Pieces of mosaics and some columns were found early in the 19th century, and some excavations were carried out later in that century, but Paolo Orsi performed the first serious excavations in 1929, and later by Giuseppe Cultrera in 1935-39. The latest major excavations were in the period 1950-60 by Gino Vinicio Gentile after which the current cover was built. Andrea Carandini has performed a few very localised excavations in the 1970s.
Sofiana can be considered as a stopping area between Catania and Agrigento. The most important discovery was a big thermal construction at the Trigona house that was discovered in the IV century, where you can see structures of Augustan origin in marble and signs of mosaics that were illegally opened that are contemporary with those of the Casale.

3. HIPERSPECTRAL DATA ACQUISITION

MIVIS (*Multispectral Infrared and Visible Imaging Spectrometer*) airborne system is undoubtedly the most interesting application in the archaeological field among the hyperspectral sensors.

MIVIS sensor (Daedalus AA5000) is a scanning system, founder of new generation of airborne hyperspectral sensors, working with a high spectral and range gating. It is a modulate tool consisting of 4 spectrometers taking simultaneously the radiation reflected by ground surface in the visible (20 bands between 0.43 and 0.83 µm), in the near-infrared radiation (8 bands between 1.15 and 1.55 µm), in the middle-infrared radiation (64 bands between 2.0 and 2.5 µm) and in the thermal infrared radiation (10 bands between 8.2 and 12.7 µm) covering totally 102 bands; besides it is characterized by a 2mrad IFOV (Instantaneous Field Of View) and 71.1° FOV (Field Of View). The sensor is housed aboard a CASA 212/200 twin-engine plane owned by Compagnia Riprese Aeree of Parma.

The aerial swaths over *Villa del Casale* and *Sofiana* sites were taken on 06/20/2002, within a photogrammetric flight plan for archaeological surveys (fig.1). Two swaths were taken at different times: the first one at about 9:30 a.m., the second at about 12:30 p.m., in order to be able to highlight, from the comparison between the relevant images, the radiometric variations due to the heating up of the ground. Each swath consists of two flight strips, North-South direction, 1500 m height; the images produced are characterized by 3 m geometric resolution and they are supplied with the only geometric correction due to the panoramic distortion induced by the sensor.

For the image calibration, using a spectroradiometer we could supply a direct survey, simultaneous to the flight, of the reflectance values (spectral signatures) of the different ground typologies in the site (fig. 2).

Figure 1. Study area

Figure 2. Direct survey of the reflectance

4. PRE-PROCESSING DATA

In this research the first 28 bands and the last 10 bands were used. For the first 28 bands the physical datum measured is the radiant emittance [W/cm^{2}sterad*µm] while the last ten bands supply temperature values obtained from a linear interpolation between the temperatures of two blackbodies kept respectively at the temperature of –15°C e +45°C within values above zero.

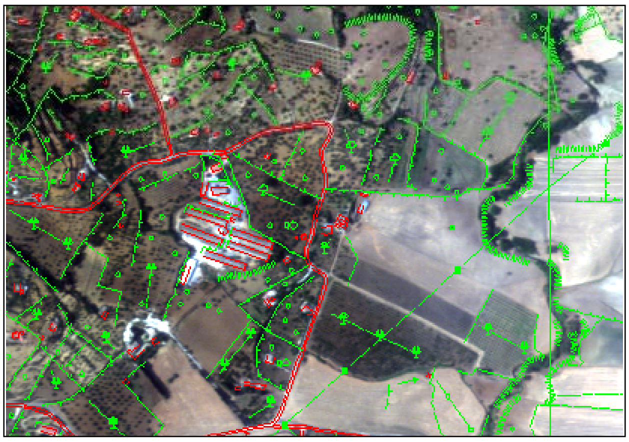

Figure 3. Regional Map overlaid on MIVIS image

As it's known, images must undergo geometric and radiometric correction. As regards geometric correction, MIVIS images are affected by distortions connected to the movement of the aircraft and the sensor characteristics (geometric distortion within FOV limits). Georeference tests have highlighted the necessity of using a lot of Ground Control Points and of splitting up each scene in subscenes with a limited extension to which to apply top-class polynomial algorithms (Rubber Sheeting). Anyway, if this approach is satisfactory from a cartographic viewpoint, it is not satisfactory from the viewpoint of the following phases of the spectral analysis; in fact, the resampling of the image pixel during georeference process modifies the spectral contents. So we have decided to refer the 12:30 image to the 9:30 one, taken as reference image, in order to resample only one image. Later, after executing all spectral analyses, the two images were georeferenced to the National Map System (Gauss-Boaga). In figure 3, the 1:10,000 Regional Map was overlaid on the georeferenced MIVIS image.

The acquired data are always affected by radiometric errors due to the sensor characteristics, to the atmosphere and to the lighting geometry. In the thermal bands these errors are displayed on the image by stripes.

The correction of these errors and the reflectance calibration are necessary in order to compare images obtained at different times, as reflectance is a physical property of the examined surface.

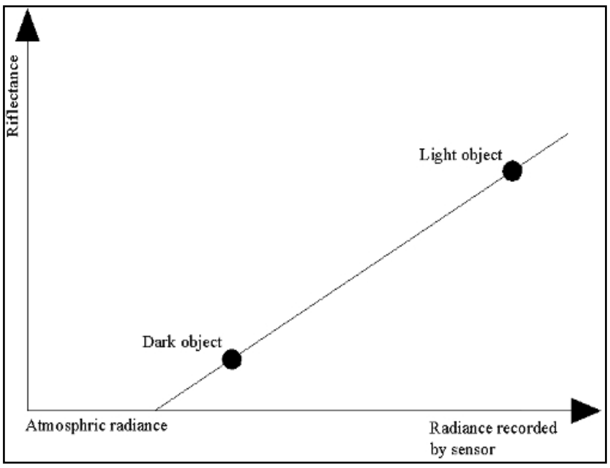

Figure 4. Calibration line

In order to get this goal, the linear empirical method was used, which uses empirical relations between radiant emittance and reflectance. This method requires the direct knowledge of the spectral signatures of a dark area and a light area, so to determine the calibration line. The intersection of this line with the axis of abscissas represents the contribution of the atmospheric radiance (fig.4).
To correct the data in thermal bands the PCA (*Principal Component Analysis*) method was used. Preliminary, PCA was applied to 10 thermal bands. This method changes the images of which DN (Digital Number) doesn't represent value of temperature. The most part of information is contained in the first principal components. In this particular case the 99.4% of the information is contained in the first four principal components and the remaining 0.6% in the last six principal components. The last six components, containing the noise, were deleted instead the remaining four components were inverted so temperature values were obtained again.

5. HIPERSPECTRAL DATA ANALYSIS

As already said, the presence of underground structures causes humidity variations in the ground. These variations affect vegetation and some physical parameters such as *Thermal Inertia* and *Thermal Conductivity*.
The distribution of vegetation in the first underground can underline regular shapes to put in touch with areas with more or less humidity. Practically you can notice that vegetation is more luxuriant in more often-vegetated ground layers and less luxuriant in reduced ground thickness, such as, for instance, where there are underground wall structures. The humidity in the top underground, due to the well-known capillarity phenomenon, moves towards the surface and, during the heating up phases, it evaporates, taking away ground and causing a temperature decrease.
The interaction of underground structures with the surface characteristics was examined by processing four parameters: *NDVI* (*Normalized Difference Vegetation Index*), *Thermal Inertia*, *Thermal Deviation*, *Thermal Conductivity.*

5.1. NDVI

The research of vegetation as an indicator for underground structures is based on the spectral response in the visible and in the near-infrared (0.8 μm). The more luxuriant vegetation and more the reflected energy increases in the near-infrared and the reflected one decreases in the red area; this characteristic causes that the difference between reflected energy in the infrared and reflected energy in the red increases proportionally to the vegetation health.
NDVI was obtained for both images in order to carry out a comparison.

$$NDVI = (\rho_{nir}-\rho_r)/(\rho_{nir}+\rho_r)$$

Arctang function was applied to the image obtained in this way: this function causes a flattening and an expansion of the image histogram, improving the contrast and making the photo interpretation easier.

5.2. Thermal Inertia

Thermal Inertia is the measurement of the response speed of a material to the temperature variations. Giving or taking away heat from a object, this object gets warm or cools down quicker than another object. Water is characterized by a high thermal inertia; this physical characteristic enables to investigate the possible presence of underground structures, because, as already said, underground structures produce variations on the underground humidity. The *Thermal Inertia* is equal to the absorbed heat divided to temperature variations;

$$I = \frac{Q}{\Delta T}$$

To calculate the quantity of heat absorption it is necessary to make some premises; the incident energy from the sun is partly reflected, partly absorbed and partly transmitted. This behaviour is set out in Kirchhoff law

$$1 = \rho + \tau + \alpha$$

where 1 represents 100% of the incident energy of the surfaces,

$\rho = \frac{E_r}{E_{inc}}$ indicates the percentage reflected

$\tau = \frac{E_t}{E_{inc}}$ indicates the percentage transmitted

$\alpha = \frac{E_a}{E_{inc}}$ indicates the percentage absorbed

For an opaque body $\tau = 0$ thus

$$1 = \rho + \alpha\,; \qquad \alpha = 1 - \rho\,; \qquad \alpha = \frac{E_a}{E_{inc}} = 1 - \rho\,;$$

$$E_a = E_{inc}(1 - \rho) \qquad \text{but} \qquad E_{inc} = \frac{E_r}{\rho}$$

$$E_a = \frac{E_r}{\rho}(1-\rho) = Q$$

E_r is the value of the radiance measured by the sensors, while the value of ρ is extracted from the images calibrated in reflectance.
This calculation was applied to the both images in order to generate two images of which DN represents the quantity of absorbed energy from the Pixel in the instant of the image's acquisition. Successively another image containing the mid value of energy absorbed was generated. This image is multiplied by the time taken to pass between the acquisitions furnishing the quantity of heat absorbed by the pixel.
The temperature variation $\Delta T = T_2 - T_1$ was calculated considering that T_2 is the average value of the 10 thermal bands of the 12:30 a.m. image and that T_1 is the average value of the 10 thermal bands of the 9:30 a.m. image.
Arctang function was applied to image obtained, containing the values of *Thermal Inertia*. Such a function stretches to a horizontal asymptote therefore easing the variability when the values of the thermal inertia are raised, giving a better contrast of images.

5.3. Thermal Deviation

Thermal Deviation is the difference between the local value of the temperature and the average value of the surrounding area. For this application the image of 9:30 a.m. was chosen because especially in the first hours of day, you can notice thermal anomalies due to different evaporation

$$\Delta T(x,y) = T(x,y) - T_m(x,y)$$

where

T(x,y) is the local value of the temperature

$T_m(x,y)$ is the average value of the surrounding area.

The dimension of the area in which you average the temperature value is chosen in relation to the deduced dimensions of the underground structure. The average value was extracted using a *convolution filter*, with a *Kernel* of 3 pixels. However in the average value, the value of the temperature of the Kernel's central pixel was not taken into account. This choice is justified by the fact that if the temperature of such pixel is not much removed from the pixel, which it calculates, that is if there are no anomalies, its value will have no relevant influence on the average value.
In the case of notable deviations, also taking into account the temperature of the central pixel, the average would be closer to the value of the central pixel temperature reducing DN value of the resulting image therefore the contrast of the image making the photointerpretation operation more difficult.

5.4. Thermal Conductivity

Thermal Conductivity is a parameter, which enables the discovery of humid areas, in which water is an optimum heat conductor. Having available the two successive elevations of temperature in the reheating stage it is possible to extract indications regarding thermal conductivity. Supposing that the image is composed of many prisms of indefinite lengths and that the lateral faces of the prism are in contact with those of the adjacent prism, under the effects of a surge of heat applied to the superficies of the prism the transmission of the heat from the lateral faces of the adjacent prisms is more or less rapidly depending on its thermal conductivity. If the conductivity is nil, the thermal *gradient G* between the prisms, dependant on the source of heat and the adjacent prisms, increases in proportion to the intensity of the heat surge.
This implies the relation between the temperature gradient and the value of the temperature of the prism, depending on the heat surge (normalized gradient G_n), is constant, independent of the intensity of the heat (A.M. Tonelli, 1997)

$$G = Abs(T(x+1,y)-T(x,y)+Abs(T(x,y+1)-T(x,y))$$
$$G_n=Abs(T(x,+1,y)-T(x,y)+Abs(T(x,y+1)-T(x,y)/T(xy)$$

Whereby if the intensity of the surge increases from t_1 to t_2 the value of the normalised gradient is maintained as a constant

$$Gn(t_1)-Gn(t_2)=0$$

For elements with a thermal conductivity other than zero, the expression takes the name *Space Temporal Variation (STV)* and assumes values as near zero as the thermal conductivity is less.
In this experimentation the *Thermal Conductivity* was calculated for both aerial swaths.

5.5. Synthesis map

The images relative to the above mentioned parameters studied were put together so one unique map was produced where lineation of the presence of humidity could be individuated. To generate this map a greater importance was given to the parameters more sensible to humidity; in particular the presence of water has a great influence on the *Thermal Conductivity*, on the *Thermal Inertia*, on the *Thermal Deviation* and less on the *NDVI*. Putting together all these considerations the following amplifying factors were chosen (Tab. 1). In figure 5 the images of some zones, which are characterised by the anomalies comparable to the possible presence of underground structures, were compared with real colour image. The *Villa del Casale* is evident within the magenta circle.
Each colour of rectangle corresponds to an area characterised by the possible presence of underground structures.

Parametro investigato	Fattore moltiplicativo
Conduttività Termica	10
Inerzia Termica	7
Scostamento Termico	5
NDVI	1

Table 1. Amplifying factors

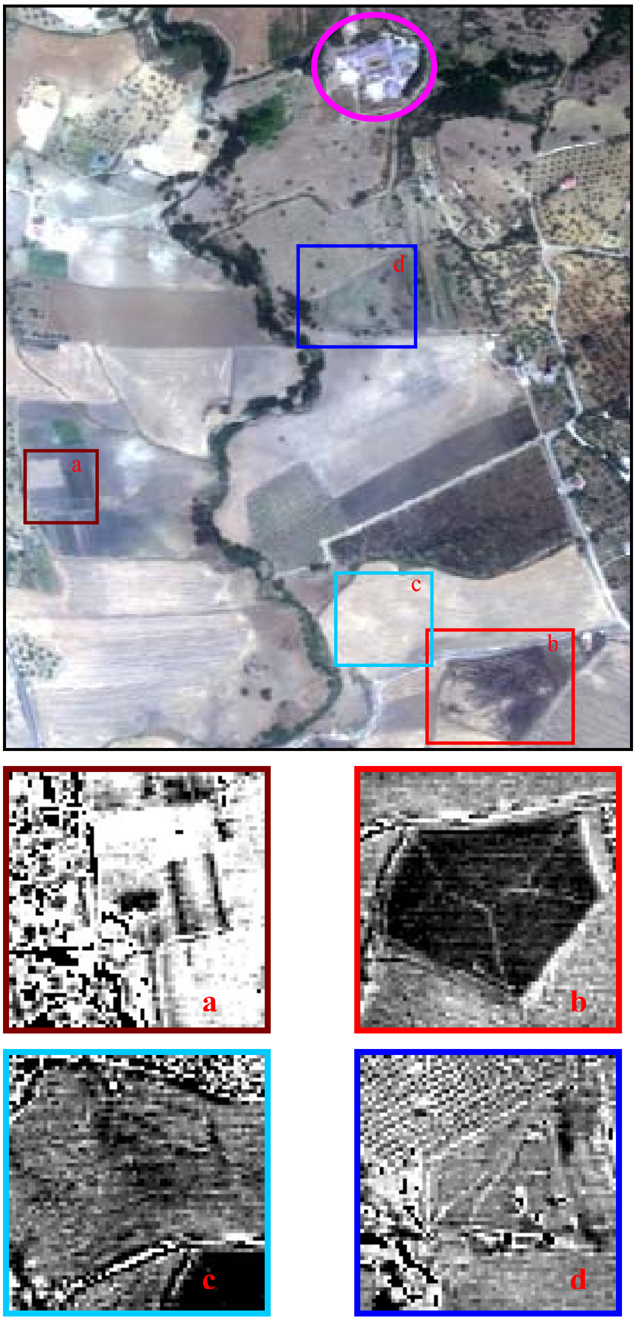

Figure 5. Zones characterised by anomalies

6. GIS DATA ANALYSIS

Using *Arcview GIS 3.2* software, the information acquired by the hyperspectral techniques were overlaid on morphologic data and on the *historical road network map*.

The testing area shows a variable morphologic state. The altimetric range is between 380 and 850 m. Interpolating the level curves of the vector Regional Map at a scale of 1:10,000 a DTM with 10 m grid-cell was generated. From DTM slope map with 3 classes was obtained: between 0% and 10%, between 10% and 20% and between 30 % and the maximum slope value in the testing area (fig.6).

Taking in consideration that the probability of finding archaeological settlements decreases if the slope increases, a numeric value was given to each slope class as higher as the class value is less. In particular to the first class was given the 10 value, to the second 6 value and to the third the 2 value.

Figure 6. Slope map

For the rebuilding of the *historical road network* the historical maps were taken in consideration (*Itinerarium Antonini e Tabula Peuntingeriana*), which give information on the principal crossing routes in the III-IV century Sicily. Those routes were crossed with the "*Regie Trazzere*" and other paths of minor importance so the location of antique routes could be conjectured, nowadays removed. P. Orsi, famous archaeologist in Sicily of the first of XIX century, wrote that: "…. *almost all the old Regie Trazzere were the bad and big roads of the Greek and Roman antiquity*". The road information is important because it is possible that along the connection roads, other archaeological settlements could be finding.

The roads individuated were digitized and a map with three classes was done. Each class contains the roads with the same historical importance; subsequently, greater is the historical importance of the classis and higher numerical value given to the class; also in this case, the values 10, 6 and 2 were chosen.

Interpolating this information a map was done in a raster format, where the nearer pixel to historical road network the higher numeric value given to the pixel (fig. 7).

All information acquired were overlaid: in particular a synthesis map relative to the *Villa del Casale* area and to *Sofiana* area, which contain hyperspectral information, the slope map and historical road network map were put together to obtain one unique map where the greater the probability to find settlements archaeological and the higher numeric value of the pixel. The figure 8 shows a particularity of the overlay of pixel, of red colour, with high probability of the presence of buried structures, in the MIVIS streak in real colours. Observing the figure two areas are characterised by a greater presence of red pixels.

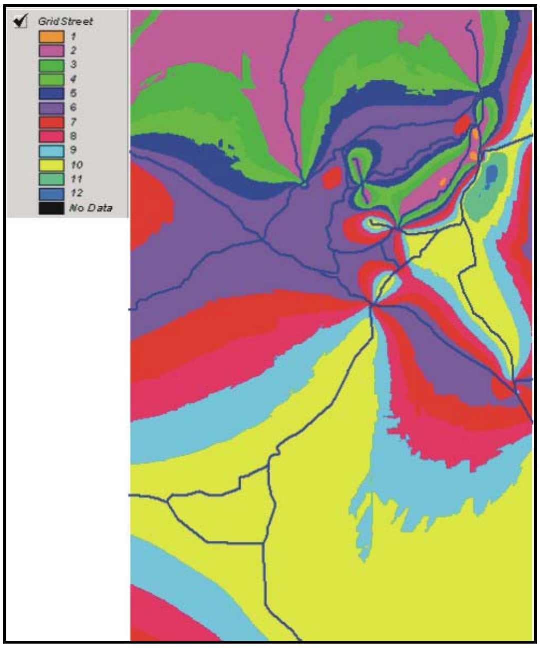

Figure 7. *Historical road network* raster map

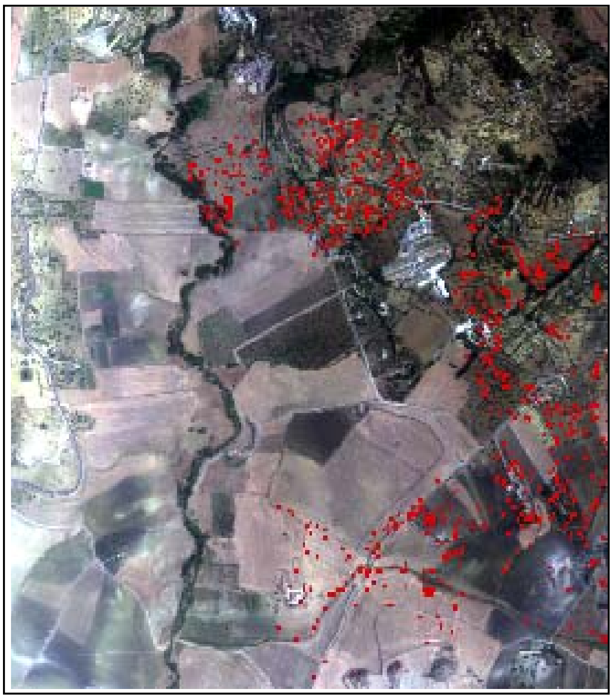

Figure 8 *Prediction map of archaeological finds* overlaid on MIVIS image

7. CONCLUSIONS

This study has shown how, by utilising the images produced by hyperspectral sensors, in particular the MIVIS sensor, it's possible to gather information, with relative speed, on the characteristics and behaviour of the soil - otherwise difficult to measure. Never the less during the image analysis, some problems emerged due principally to the geometric resolution but also to notable geometric distortions thus conditioning the successive operations of subtraction and addition between the images. The geometric resolution above all influences the dimension of each object that it is possible to discriminate in the images. In particular, for this study, the images have a geometric resolution of 3 meters; therefore it was not possible to discover underground sites with a dimension inferior to 3 metres.

The integration of the hyperspectral data with morphologic data and information about *historical road network* allows to generate a *Prediction map of archaeological finds*.

This map gives only probabilistic information that should be validated by the use of other types of investigation like geophysical ones. The georadar technique is one of the newer techniques that is most frequently used for geophysical work in different fields. The georadar survey is based on the study of the behaviour that electromagnetic waves have when they propagate through materials with different dielectric properties. In particular, it can be, successfully, used to detect geological structures, carsick cavities, gas lines, or archaeological structures. Measurements were carried out with the new GSSI (Geophysical Survey System, Inc.) georadar system, namely SIR3000. In this case, georadar acquisition was carried out using a 400 MHz antenna, best suited for the type of research here discussed and the depths that we planed to reach.

In this experimentation, the geophysical research was done on the zone indicated in figure 5 with the letter (d) characterized by a big value of probability. The area was detected by the acquisition technique aimed at the rendering of the, so-called, "time-slices" representation. The "time slices" technique is used in many georadar applications to produce a graphic representation of profiles. This technique represents one of several ways of carrying out reflection tomography and allows us to reconstruct, through horizontal sections, the planimetric behavior of the reflections that are produced by underground electromagnetic discontinuities.

In particular 16 parallel profiles in North - South direction and 11 parallel profiles in East - West direction were acquired. The acquired data were processed by Reflex software, using standard function in order to remove random and coherent noise.

The geophysical measurements have confirmed the presence of anomalies referable to buried structures. In figure 9 the result of the geophysical research is represented: the red areas are characterized by discontinuities due to the presence of buried structures. The figure 10 shows the overlay of the red areas, individuated with geophysical techniques, on white sign, individuated on the synthesis image obtained with hyperspectral techniques.

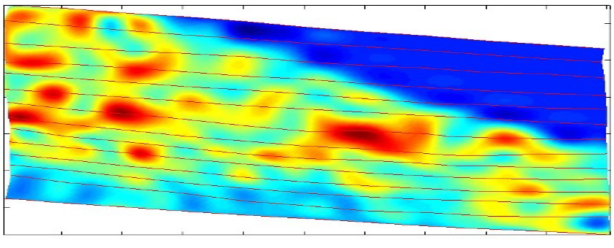

Figure 9. Chart of geophysical research result

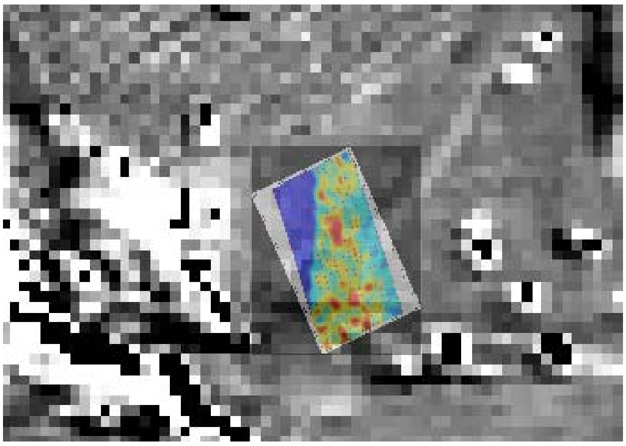

Figure 10. Overlapping of geophysical chart on the synthesis image

REFERENCES

Disceglie S., 1984. La termografia della prospezione archeologica applicazioni sull'acropoli di Egnazia. In: SITE Società italiana per il telerilevamento, Rome, Italy.

Ebert J.I., 1984. *Remote Sensing Applications in Archaeology*. In: Advances in Archaeological Method and Theory 7, pp.293-362.

Holma A. 1901. Storia della Sicila nell'antichità vol. III (Itinerarium Antonini), Torino.

Orsi P., 1978. *Una storia accademica*. In Archivio Storico per la Sicilia Orientale, LXXIV, pp. 465-571.

Scollar I., A. Tabbagh, A. Hesse, I, Herzog, 1990. *Archaeological prospecting and remote sensing*, Cambridge University Press.

Sereni E., 1961. *Storia del paesaggio agrario italiano*. Laterza, Bari, pp.37-39.

Sicca U., 1924. *Grammatica delle iscrizioni doriche della Sicilia*, Arpino.

Tonelli A.M., 1997. *Complementi di telerilevamento.* LUNI, Italy.

Tonelli A.M., 1974. Trattamento analogico di informazioni provenienti da telesensori termici. In: *Atti Congresso dell'Associazione Elettrotecnica Italiana*.

Tonelli A.M., 1972, Termografie all'infrarosso da stazioni a terra e dall'aereo. *Quaderni della ricerca scientifica*, pp.83.

Uggeri G.. 1982/83. La viabilità romana in Sicilia con particolare riguardo al III e IV sec. d.c (Tabula Peutingeriana), Kokalos, voll. 28/29 pp. 424-460.

ACKNOWLEDGEMENTS

We would like to thank:

- Prof. Pietro Cosentino, Dr. Patrizia Capizzi, Dr Paolo Messina and Gianluca Fiandaca from Dipartimento di Geofisica of Palermo University for geophysics survey operations;
- Arch. Laura Riccobono from Dipartimento di Rappresentazione of Palermo University for her valuable contribution to the compilation of *historical road network map.*